Journal of Materials Chemistry C

Accepted Manuscript

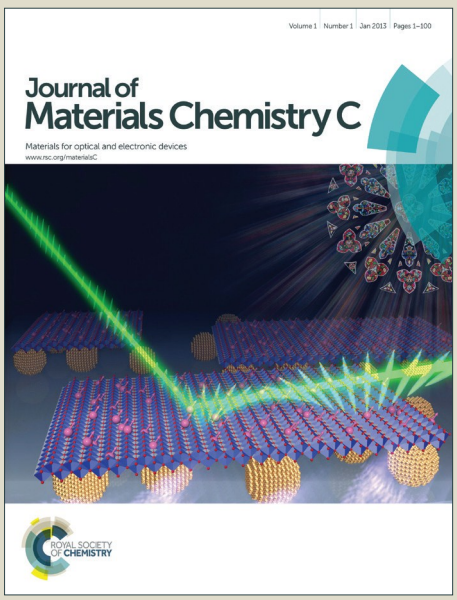

ROYAL SOCIETY OF CHEMISTRY

www.rsc.org/materialsC

Journal Name

RSCPublishing

ARTICLE

Facile Growth of Centimeter-Size Single-Crystal Graphene on Copper Foil at Atmospheric Pressure

Cite this: DOI: 10.1039/xoxxoooooox

Received ooth January 2012,
Accepted ooth January 2012

DOI: 10.1039/xoxxoooooox

www.rsc.org/

Jing Li, [ab] Xuan-Yun Wang, [c] Xing-Rui Liu, [ab] Zhi Jin, [c] Dong Wang*[a], Li-Jun Wan*[a]

By mildly oxidizing Cu foil and slowing down total gas flow rate, we develop an easily repeatable atmospheric growth method to grow single-crystal graphene of centimeter-size. The graphene edge, which is different from previously reported straight edge, is connected by a series of graphene-corner. The graphene-corner, ranging between 100˚ to 110˚, is formed by a Zig-Zag edge and a Mix edge. The oxidation of Cu crystal boundaries results in the rearrangement of active Cu site for graphene nucleation, thus suppressing graphene nucleation density.

1 Introduction

Due to the outstanding physical properties, such as ultrahigh carrier mobility, thermal conductivity, and tensile strength, graphene has attracted increasing attention for both fundamental science and technological applications.[1] Chemical vapor deposition (CVD) is currently the only approach to grow large-scale high quality graphene.[2] However, the ordinary CVD graphene is polycrystalline,[3] which is stitched together with disordered grain boundaries. Both theoretical simulation and experiment result have demonstrated that the electrical transport property or quality of polycrystalline graphene is worse than mechanical exfoliated graphene.[4] At the same time, it has been reported the property of CVD graphene within a single domain is comparable with the exfoliated sample.[5] Thus, growing large-size single-crystal graphene (SCG) without grain boundaries becomes a great challenge for further promoting the practical application of graphene in large-scale functional electronic, photonic and mechanical devices.[6]

So far, a variety of substrates such as noble or transition metals[7], dielectric substrate[8] and semiconductor substrates[9, 10] have been reported to grow SCG. For example, epitaxial growth of SCG has been realized by coalescing alignment-determined graphene nucleation on hexagonal boron nitride[9] and germanium[10] substrates. Cheng et al. reported repeated etching-growth cycle to grow SCG of millimeter-size on Pt.[11] Considering the relatively low price of commercial Cu foil, CVD growth of SCG on Cu substrate is an expectably promising way to bring about the practical applications of high quality and large-size graphene. Generally speaking, the most important strategy to grow large-size SCG on metal substrate is to reduce the graphene nucleation density and thus increasing the size of SCG. So far a number of methods have been developed to reduce the nucleation density. Firstly, the substrate smoothing methods such as physical[12, 13] and electrochemical polishing,[14] Cu re-solidifying,[15] can effectively reduce the nucleation sites on Cu surface. Secondly, optimization of CVD condition, including gas contents[11, 16], growth pressure[17], vapor trapping,[18, 19] can modulate the growth kinetics and thus prompt the growth of SCG. Recently, Cu substrate oxidation method has been proven to be an effective method to suppress graphene nucleation, [17, 20, 21] although the exact mechanism for the oxidation method is still under debate. As LP(low-pressure) CVD condition can result in lower graphene nucleation density[10] and more easily gas switching[20], most of the SCG with large size were grown under LP. For example, the size of ~1 cm SCG was obtained on oxygen-rich Cu substrate under LP,[20] and the largest SCG size of atmospheric pressure (AP) CVD on Cu substrate is 5.9 mm.[21] However, high vacuum growth condition needs high maintenance cost[2]. Besides, most of the ever-reported SCG growth methods contain tedious pretreatment and annealing process, which might further increase the diffulty for popularization and application. Consequently, developing a facile and practical APCVD method to grow large size SCG is still a hot pursuit.

Herein, we report a facile APCVD method to synthesize centimeter-scale SCG on commercial Cu foil. This method does not need special pre-treatment nor the involvement of extra O_2 switching step. The quality and crystallinity of obtained centimeter-scale graphene has been characterized by scanning probe microscopy, Raman, selected area electron diffraction (SAED) and the graphene based field-effect transistor (FET). Interestingly, the as-obtained graphene edge is found to be formed by a series of graphene-corner (GC) ranging from 100° to 110° by statistics. Finally, the detailed influence of Cu oxidation and gas flow rate on graphene nucleation suppression is investigated by scanning electron microscopy (SEM), energy dispersive spectroscopy (EDS) and backscatter electron diffraction (EBSD).

2 Experimental methods and characterization

2.1 Materials and graphene growth

As shown in Fig. 1a, commercial copper foil (99.8% purity, 25 μm thick, Alfa-Aesar) was used as substrate for the CVD graphene growth. After a brief sonication in HCl (~10%, for 10 minutes) and $(NH_4)_2S_2O_8$ (~0.1M, for 3 minutes) aqueous solution, respectively, to remove surface contamination and coating layer, the copper foil of 1.5 × 5 cm^2 size was inserted into an one-inch corundum tube furnace and heated in high purity Argon atmosphere (the oxygen concentration is about 3 ppm) to mildly oxidize the Cu surface, and then a small amount of hydrogen was introduced to reduce the Cu oxide (this step does not affect nucleation density of graphene, but is important to avoid Cu over-oxidizing and etching, as in Fig. S1†). When the growth temperature reached 1075 °C, the gas was adjusted to the ratio labeled in Figure 1a to maintain graphene growth.

Firstly, we study the influence of total gas flow rate on the graphene nucleation density on Cu foil. The graphene was grown under different gas flow rate while with keeping other experiment parameters the same, and the growth was stopped till the graphene edge began to merge. After growth and cooling down, the Cu foil was heated in air for about 2 minutes at 200 °C to make graphene optically visible,[22] and then the relationship between gas flow rate and graphene nucleation density was obtained by statistics (Fig. 1b). Optical photographs (Fig. S2†) of graphene on Cu indicate that as gas flow rate increases, both the growth rate (Fig. S3†) and nucleation density (Fig. 1b) increase. With the balanced consideration of graphene growth rate and nucleation number, the gas flow rate of 100 standard cubic centimeters per minute (sccm) is chosen for the large-size graphene growth. By extending growth time to about 10 h, the hexagonal graphene of centimeter-scale is obtained (Fig. 1c).

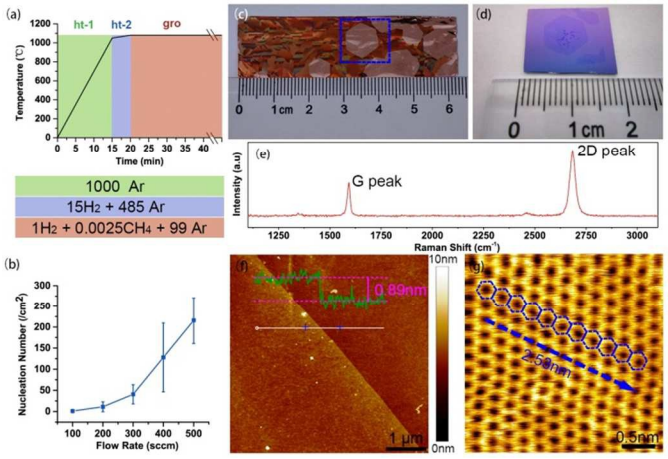

Fig. 1 (a) Process diagram of graphene growth on Cu substrate. The gas content and flow rate in each growth stage is mark by the lower insert with the unit of sccm. (b) The mean graphene nucleation number as a function of total gas flow rate. Optical photograph of centimeter hexagonal graphene (bright color) on Cu substrate (c), and the graphene of blue dashed rectangle zone in panel (c) that was transferred onto SiO_2/Si substrate (d). (e) Typical Raman spectra of graphene on SiO_2/Si substrate. (f) The AFM image of graphene edge on SiO_2/Si substrate. The vertical height variation along the white line is inserted as green line and the graphene edge thickness is labelled in panel (f). (g) The STM image of graphene on Cu substrate. The hexagonal unit is marked by blue dashed hexagon, and the length of ten neighboring hexagonal units is labelled in panel (g).

2.2 Transfer of graphene

The transfer of CVD graphene onto SiO_2/Si substrate or TEM grid was performed with the PMMA (polymethyl mechacrylate) assisted transfer method as reported previously.[23] It is worth mentioning that, compared with polycrystalline graphene, SCG is more easily to fold or break when dissolving PMMA layer. Thus, after picked up by target substrate, the graphene should be dried under higher temperature and longer time.

2.3 Characterization

The graphene morphology was characterized with field-emission scanning electron microscopy (SEM, JEOL 6701F, 5kV) on Cu. The structure characterization was performed by Raman spectroscopy (Thermo Scientific DXR, 532 nm laser wavelength) on SiO_2/Si substrate and field-emission transmission electron microscopy (TEM, JEOL 2011F, 200kV). The graphene structure and thickness was studied by scanning probe microscopy [atomic force microscopy (AFM, Veeco Multimode) and scanning tunneling microscopy (STM, Agilent Technologies)]. The Cu crystal phase was identified by a scanning electron microscopy (SEM, ZEISS-MERLIN) equipped with an electron backscatter diffraction (EBSD, Oxford Instrument, 10kV).

3 Results and discussion

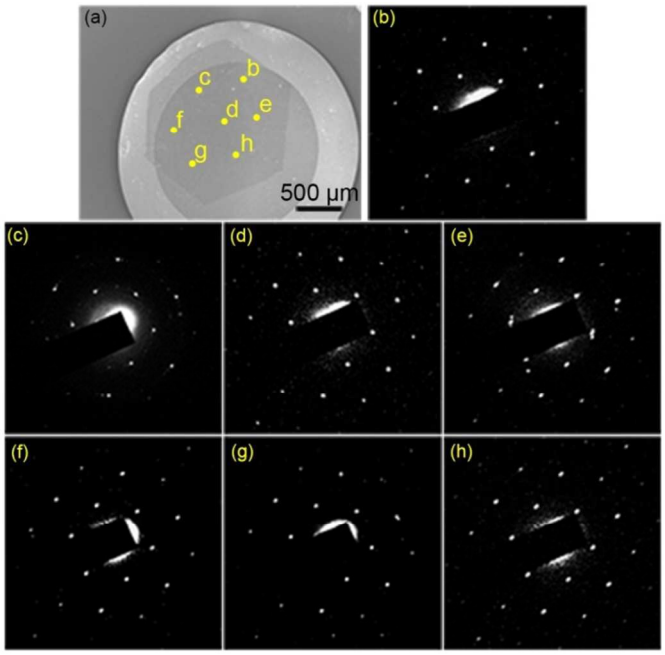

Fig. 2 (a) SEM image of a ~ 2 mm hexagonal graphene domain transferred onto TEM grid. (b-h) Some representative SAED patterns taken from different holes of the TEM grid relative to the approximate location labelled in panel (a).

To confirm the graphene thickness, the graphene was transferred onto the SiO_2/Si substrate and characterized by optical microscopy, Raman spectroscopy and scanning probe microscopy. The color contrast of the graphene flake is uniform in most area of the optical image (Fig. 1d), except for some darker hexagonal spot, which is ascribed to multilayer graphene (Fig. S4†). Raman spectra were collected on the graphene flake arbitrarily, and the typical graphene Raman spectra is given as Figure 1e. The intensity ratio of I_{2D}/I_G is higher than 2, and the full width of half maximum 2D peak is about 33 cm^{-1}, indicating that predominantly monolayer graphene is grown on Cu foil.[23, 24] In addition, atomic force microscopy (AFM) image

reveals that the graphene is of uniform thickness, and the height of graphene edge is about 0.89 nm (Fig. 1f) , which is in consistent with the result of PMMA-transferred monolayer graphene.[25] The high-resolution scanning tunneling microscopy (STM) image shown in Figure 1g reveals honeycomb structure with the distance of adjacent benzene unit of about 0.25 nm, which perfectly matches the characteristic STM image for single-layer graphene.[26]

The crystallinity structure of as obtained hexagonal graphene is characterized by transmission electron microscopy (TEM) and selected area electron diffraction (SAED). The graphene growth process was stopped at the growth time of 2 h to obtain the hexagonal graphene of ~2 mm size. Then, this graphene flake was transferred onto the TEM grid as shown in Figure 2a. A series of surveys on graphene domain was obtained by SAED on the graphene sample arbitrarily.[27] Seven representative SAED patterns are provided in Figure 2b-h. About 5 batches of graphene samples and more than 200 SAED patterns were randomly collected, and each hexagonal graphene shows uniform six-fold symmetrical SAED patterns including some multi-layer structure (Fig. S5†), which confirming that the hexagonal graphene is single crystalline structure across the entire hexagonal flake.[18] Besides, the carrier mobility of the hexagonal graphene film was tested to be ~3500 $cm^2V^{-1}S^{-1}$ (Fig. S6†), which is higher than that of the polycrystalline graphene device obtained at the same device fabrication condition.[23]

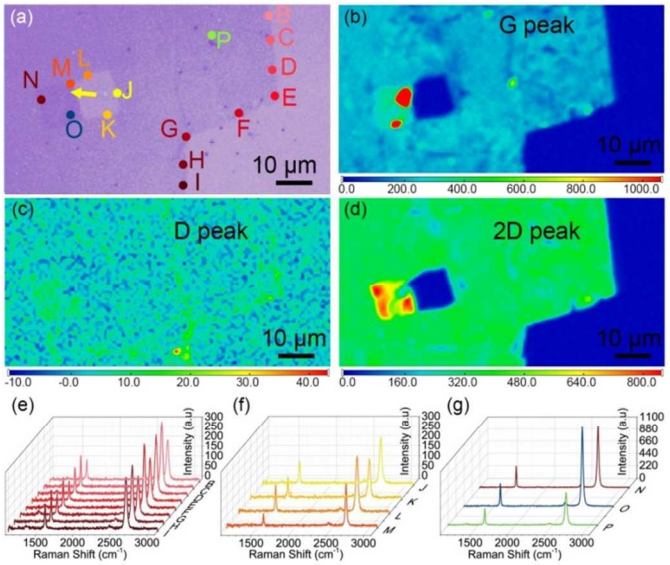

Fig. 3 Raman spectroscopy characterization of graphene domains transferred onto SiO_2/Si substrate. (a) Optical microscopy taken from the edge of one graphene domain. (b) Raman maps of G peak (b), D peak (c) and 2D peak (d). (e) Raman spectra of graphene grown edge with respect to the spots form B to I in panel (a). (f) Raman spectra of graphene edge which was torn by transferred process. (g) Raman spectra of graphene on SiO_2/Si substrate (spot of P) and suspending graphene (spots of N and O).

To further investigate the quality of the graphene and edge structure, Raman maps of I_G, I_{2D} and I_D intensity were collected and shown in Figure 3a-d, respectively. The step size was 1 μm, and the investigated region was 90 × 50 $μm^2$. The maps present uniform G (1592 cm^{-1}) , D (1346 cm^{-1}) and 2D (2684 cm^{-1}) peak of the graphene flake, except for some graphene folds, which might be brought about by the high growth temperature (Fig. S7†) or transfer process.[28] The I_{2D} is more than twice as strong as I_G, indicating monolayer graphene coverage in the whole investigated region.

It is worth mention that I_D is negligibly weak over the whole graphene film (Fig. 3c), including the graphene growth edge (the average intensity ratio of I_D/I_G from spot B to I is about 0.1, Fig. 3e) and the irregular edge (the average intensity ratio of I_D/I_G of spot K and L is about 0.05, Fig. 3f) which was torn by transfer process. However, the intensity ratio of I_D/I_G of spot P is about 0.1, which is obviously higher than that of spots N and O (the average intensity ratio of I_D/I_G is 0.02). Considering the transfer process and substrate influence, the Raman intensity of I_D and I_G is not intuitive enough to demonstrate the graphene edge structure. Besides, the GC of spot E is obviously deviated from 120°,[12] and the graphene edge cannot be both of Zig-Zag (ZZ) at the same time.[29, 30]

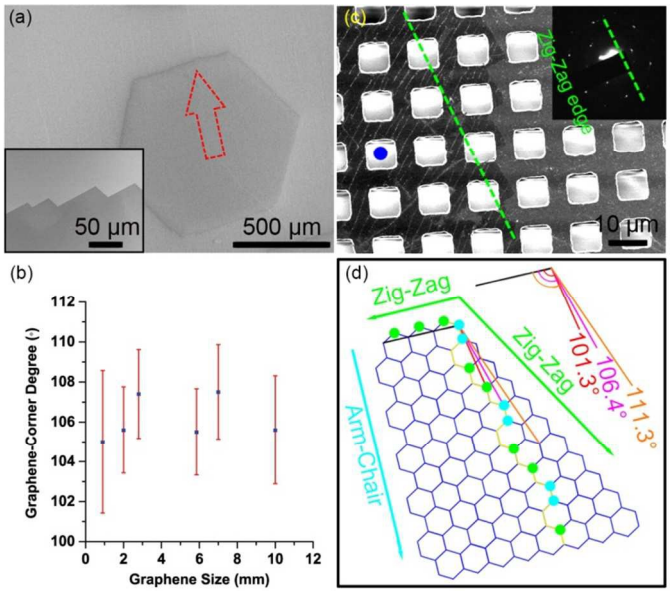

Fig. 4 (a) Typical SEM image of one graphene domain on Cu substrate. Bottom left: Enlarged SEM image of the graphene edge marked by red arrow in panel (a). (b) The statistics of mean GC degree relative to the graphene size. (c) The SEM image of a graphene edge transferred onto TEM grid, and the up insert is the SAED pattern of the graphene marked by blue spot. The green dashed line indicates the ZZ edge direction determined by the SAED pattern. (d) Schematic illustration of the edge structure of GC with the angle between 100° to 110°. The ZZ edge and AC edge direction are marked by green and cyan arrows, respectively. One of the MX edge is highlighted by yellow line in panel (d), in which the ZZ site and AC site are marked by green and cyan spots, respectively.

To further investigate the edge structure of GC, the graphene of various sizes from 10 μm (Fig. S8†) to 1 cm that obtained by our method was investigated. Interestingly, different from the straight edge as previously reported,[15, 17, 21] the graphene edge is formed by a series of GC as shown in Fig. 4a. As presented in Fig. 4b, the degree of GC ranges between 100° to 110° and shows no dependence on the graphene size. Typically, the hexagonal graphene is exclusively bounded by either ZZ or Armchair (AC) edges. Considering the intermediate stabilities, the stable graphene edge is pure ZZ structure with the corner angle of 120° in most cases.[30] Though graphene wrinkles and folds (Fig. S7†) can distort graphene initial structure to some

extent, the wrinkles and folds trend to be randomly distributed thus cannot result in statistics uniform GC distribution. To identify the corner structure, the graphene was observed (Figure S9) by SAED after transferred onto TEM grid. The angle between the long side of GC and the ZZ direction determined by SAED[31] falls in the range of ± 5° (Fig. 4c). Considering the Cu surface waviness and the transfer process, this degree deviation is acceptable to conclude the long side of GC is ZZ edge, and the other short edge is the mix structure (MX) composed of both ZZ and AC sites. The possible structure of the MX edge is revealed as the yellow line shows in Fig. 4d, in which the ZZ sites and AC sites are marked by green and cyan spots, respectively. As the GC can be repeatedly observed in the whole graphene growth process, we suppose both the ZZ edge and MX are stable structure in the growth process.[32]

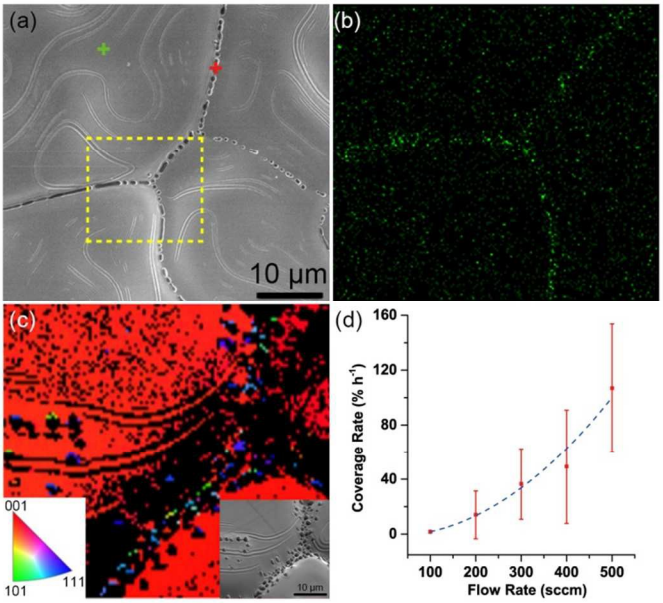

Fig. 5 (a) SEM image of Cu surface morphology after heated in Argon. (b) The EDS maps of O element of the zone marked by yellow dashed rectangle in panel (a). (c) EBSD map taken over the Cu surface as shown in the bottom right insert SEM image. Bottom left is the key orientation color map. (d) Gas flow rate dependent increment per hour of graphene coverage. The collected data are plotted as red squares, and the blue dashed curve shows the quadratic fitting curve of statistical coverage increment of graphene domain with gas flow rate.

Previous reports about SCG growth in LPCVD condition have suggested that the substrate oxidation plays a key role for grapheme nucleation suppression.[20] In the present APCVD protocol, the trace amount of oxygen in Ar (~3 ppm) may also result in the Cu oxidation. The influence of oxidation on graphene nucleation suppression is investigated by SEM, EDS and EBSD. As represented in Fig. 5a, after heating Cu foil in high purity Argon flow, some clusters of 500-1000 nm come into being mainly at the Cu crystal boundaries as well as a minority of Cu crystal surface.[33] The EDS mapping of O element in Fig. 5b (EDS spectroscopy of individual spots are shown in Figure S10) proves the O element is mainly concentrated on the Cu crystal boundary clusters (These clusters should be cuprous oxide particles as reported previously[20,21]). EBSD of Cu crystal boundaries shows that Cu atom arrangement in the cluster is different from that of Cu surface (Fig. 5c). We note that the clusters become embedded into the Cu surface and the surface becomes featureless (Fig. S11†) right after the subsequential introduction of reduction environment (CH_4/H_2). After oxidation and reduction, the Cu atoms of active Cu crystal boundaries rearrange into less active structure,[20] thus the graphene nucleation density can be well decreased after Cu surface oxidation. It is worth mentioning that the clusters at the domain boundaries after annealing step is different from the nucleation nanoparticles which are present on the surface after the reduction process, as proposed by Luo et al.[21] More control experiments were carried out to reveal the relationship between Cu surface oxidation and graphene nucleation suppression. Increasing oxygen content from 3 to 500 ppm or increasing heating time from 15 min to 12 h result in the fully oxidation of the whole Cu surface (Fig. S12†), but little improvement on decreasing graphene nucleation density. The result further proves that the clusters are not the major contributor for graphene nucleation in the present APCVD protocol.

As shown in Fig. 1b, the gas flow rate is another key parameter to control nucleation density. To have a better understanding about the influence of gas flow rate, we construct a mathematical model to mimic the growth kinetics of graphene growth under slow gas flow rate. In order to establish a simple kinetics model of graphene growth, we assume that (1) the boundary layer of gas flow on Cu surface is steady gas flow; (2) the diffusion of carbon species is much slower than the carbon reaction under the slow gas flow rate and high growth temperature. Based on these assumptions, the graphene coverage is proportional to the amount of carbon that can react on Cu surface. The equation is as following[34]:

$$S_{graphene-coverage} \propto F_{mass-transport} = [\frac{K_s h_g}{(K_s+h_g)}]C_g \qquad (1)$$

Where the $S_{graphene\text{-}coverage}$ is graphene coverage on Cu substrate; the $F_{mass\text{-}transport}$ is the flux of active species onto Cu surface; h_g is the mass transport coefficient; K_s is the surface graphene reaction constant; C_g is the concentration of gas in the bulk tube. Considering the growth temperature is higher than 1000 ˚C ($K_s >> h_g$), the equation can be simplified into $S_{graphene\text{-}coverage} \propto h_g C_g$, and the $h_g \sim P^{-1} \cdot T^{3/2}$ according to Fick's law.[35] In addition, according to Bernoulli principle[36], the fluid flows within the same elevation can be given as:

$$C_{constant} = P + \frac{1}{2} \cdot \rho \cdot v^2 \qquad (2)$$

Where P is the fluid pressure; v is the fluid flow rate and ρ is the density of fluid. Then the relationship between graphene coverage and gas flow rate can be $S_{graphene\text{-}coverage} \sim v^2$, which is consistent with the result in Fig. 5d, and proving the growth is a dynamic steady and gas diffusion determined kinetic process.[20]

Conclusions

In conclusion, centimeter-size hexagonal graphene has been synthesized on the Cu substrate by heating in Argon atmosphere and growing under low gas flow rate at AP. Raman spectroscopy, scanning probe microscopy and SAED results prove that the graphene is of single-crystalline and mainly of monolayer. The graphene edge is composed of GC, which is different from previously reported straight ZZ edge. The GC ranges between 100˚ to 110˚ and is formed by a ZZ edge and MX edge. The oxidation of Cu crystal boundaries results in the passivation of active Cu site for graphene nucleation, thus suppressing graphene nucleation density. The growth of centimeter SCG under AP condition provides an effective method to obtain high quality graphene with minimized

graphene boundaries, which is important to the electrical device application of graphene-based materials.

Acknowledgements

This work was supported by the National Key Project on Basic Research (Grants2011CB808701, 2011CB932304), National Natural Science Foundation of China (21127901, 21233010, 21433011, 21373236), and the Strategic Priority Research Program of the Chinese Academy of Sciences (Grant No. XDB12020100).

Notes and references

[a] Key Laboratory of Molecular Nanostructure and Nanotechnology and Beijing National Laboratory for Molecular Sciences, Institute of Chemistry, Chinese Academy of Sciences (CAS), Beijing 100190, P.R. China.

[b] University of CAS, Beijing100049, P. R. China.

[c] Institute of Microelectronics, Chinese Academy of Sciences, Beijing 100029, P. R. China.

† Electronic Supplementary Information (ESI) available: SEM and FET device characterization. See DOI: 10.1039/b000000x/

1. K. S. Novoselov, V. I. Falko, L. Colombo, P. R. Gellert, M. G. Schwab and K. Kim, *Nature*, 2012, **490**, 192.
2. S. Bae, H. Kim, Y. Lee, X. Xu, J.-S. Park, Y. Zheng, J. Balakrishnan, T. Lei, H. Ri Kim, Y. I. Song, Y.-J. Kim, K. S. Kim, B. Ozyilmaz, J.-H. Ahn, B. H. Hong and S. Iijima, *Nat Nano*, 2010, **5**, 574.
3. A. W. Tsen, L. Brown, R. W. Havener and J. Park, *Accounts of Chemical Research*, 2012, **46**, 2286.
4. A. W. Cummings, D. L. Duong, V. L. Nguyen, D. Van Tuan, J. Kotakoski, J. E. Barrios Vargas, Y. H. Lee and S. Roche, *Advanced Materials*, 2014, **26**, 5079.
5. Q. Yu, L. A. Jauregui, W. Wu, R. Colby, J. Tian, Z. Su, H. Cao, Z. Liu, D. Pandey, D. Wei, T. F. Chung, P. Peng, N. P. Guisinger, E. A. Stach, J. Bao, S.-S. Pei and Y. P. Chen, *Nat Mater*, 2011, **10**, 443.
6. Z. Yan, Z. Peng and J. M. Tour, *Accounts of Chemical Research*, 2014, **47**, 1327.
7. Y. A. Wu, Y. Fan, S. Speller, G. L. Creeth, J. T. Sadowski, K. He, A. W. Robertson, C. S. Allen and J. H. Warner, *ACS Nano*, 2012, **6**, 5010.
8. J. Chen, Y. Guo, L. Jiang, Z. Xu, L. Huang, Y. Xue, D. Geng, B. Wu, W. Hu, G. Yu and Y. Liu, *Advanced Materials*, 2014, **26**, 1348.
9. W. Yang, G. Chen, Z. Shi, C.-C. Liu, L. Zhang, G. Xie, M. Cheng, D. Wang, R. Yang, D. Shi, K. Watanabe, T. Taniguchi, Y. Yao, Y. Zhang and G. Zhang, *Nat Mater*, 2013, **12**, 792.
10. J.-H. Lee, E. K. Lee, W.-J. Joo, Y. Jang, B.-S. Kim, J. Y. Lim, S.-H. Choi, S. J. Ahn, J. R. Ahn, M.-H. Park, C.-W. Yang, B. L. Choi, S.-W. Hwang and D. Whang, *Science*, 2014, **344**, 286.
11. T. Ma, W. Ren, Z. Liu, L. Huang, L.-P. Ma, X. Ma, Z. Zhang, L.-M. Peng and H.-M. Cheng, *ACS Nano*, 2014, **8**, 12806.
12. Z. Yan, J. Lin, Z. Peng, Z. Sun, Y. Zhu, L. Li, C. Xiang, E. L. Samuel, C. Kittrell and J. M. Tour, *ACS Nano*, 2012, **6**, 9110.
13. L. Brown, E. B. Lochocki, J. Avila, C.-J. Kim, Y. Ogawa, R. W. Havener, D.-K. Kim, E. J. Monkman, D. E. Shai, H. I. Wei, M. P. Levendorf, M. Asensio, K. M. Shen and J. Park, *Nano Letters*, 2014, **14**, 5706.
14. Z. Luo, Y. Lu, D. W. Singer, M. E. Berck, L. A. Somers, B. R. Goldsmith and A. T. C. Johnson, *Chemistry of Materials*, 2011, **23**, 1441.
15. A. Mohsin, L. Liu, P. Liu, W. Deng, I. N. Ivanov, G. Li, O. E. Dyck, G. Duscher, J. R. Dunlap, K. Xiao and G. Gu, *ACS Nano*, 2013, **7**, 8924.
16. I. Vlassiouk, M. Regmi, P. Fulvio, S. Dai, P. Datskos, G. Eres and S. Smirnov, *ACS Nano*, 2011, **5**, 6069.
17. H. Zhou, W. J. Yu, L. Liu, R. Cheng, Y. Chen, X. Huang, Y. Liu, Y. Wang, Y. Huang and X. Duan, *Nat Commun*, 2013, **4**.
18. S. Chen, H. Ji, H. Chou, Q. Li, H. Li, J. W. Suk, R. Piner, L. Liao, W. Cai and R. S. Ruoff, *Advanced Materials*, 2013, **25**, 2062.
19. Y. Zhang, L. Zhang, P. Kim, M. Ge, Z. Li and C. Zhou, *Nano Letters*, 2012, **12**, 2810.
20. Y. Hao, M. S. Bharathi, L. Wang, Y. Liu, H. Chen, S. Nie, X. Wang, H. Chou, C. Tan, B. Fallahazad, H. Ramanarayan, C. W. Magnuson, E. Tutuc, B. I. Yakobson, K. F. McCarty, Y.-W. Zhang, P. Kim, J. Hone, L. Colombo and R. S. Ruoff, *Science*, 2013, **342**, 720.
21. L. Gan and Z. Luo, *ACS Nano*, 2013, **7**, 9480.
22. C. Jia, J. Jiang, L. Gan and X. Guo, *Sci. Rep.*, 2012, **2**.
23. J. Li, H. Ji, X. Zhang, X. Wang, Z. Jin, D. Wang and L.-J. Wan, *Chemical Communications*, 2014, **50**, 11012.
24. A. C. Ferrari, J. C. Meyer, V. Scardaci, C. Casiraghi, M. Lazzeri, F. Mauri, S. Piscanec, D. Jiang, K. S. Novoselov, S. Roth and A. K. Geim, *Physical Review Letters*, 2006, **97**, 187401.
25. L. Liu, H. Zhou, R. Cheng, W. J. Yu, Y. Liu, Y. Chen, J. Shaw, X. Zhong, Y. Huang and X. Duan, *ACS Nano*, 2012, **6**, 8241.
26. X. Chen, S. Liu, L. Liu, X. Liu, X. Liu and L. Wang, *Applied Physics Letters*, 2012, **100**, 163106.
27. D. Geng, B. Wu, Y. Guo, L. Huang, Y. Xue, J. Chen, G. Yu, L. Jiang, W. Hu and Y. Liu, *Proceedings of the National Academy of Sciences*, 2012, **109**, 7992.
28. X. Li, Y. Zhu, W. Cai, M. Borysiak, B. Han, D. Chen, R. D. Piner, L. Colombo and R. S. Ruoff, *Nano Letters*, 2009, **9**, 4359.
29. Z. Luo, S. Kim, N. Kawamoto, A. M. Rappe and A. T. C. Johnson, *ACS Nano*, 2011, **5**, 9154.
30. H. Shu, X. Chen, X. Tao and F. Ding, *ACS Nano*, 2012, **6**, 3243.
31. T. Ma, W. Ren, X. Zhang, Z. Liu, Y. Gao, L.-C. Yin, X.-L. Ma, F. Ding and H.-M. Cheng, *Proceedings of the National Academy of Sciences*, 2013, **110**, 20386.
32. J. Gao, J. Zhao and F. Ding, *Journal of the American Chemical Society*, 2012, **134**, 6204.
33. Y. Zhu, K. Mimura, S.-H. Hong and M. Isshiki, *Journal of The Electrochemical Society*, 2005, **152**, B296.
34. S. Bhaviripudi, X. Jia, M. S. Dresselhaus and J. Kong, *Nano Letters*, 2010, **10**, 4128.
35. E. R. Gilliland, *Industrial & Engineering Chemistry*, 1934, **26**, 681.
36. G. K. Batchelor, *An introduction to fluid dynamics*, University Press, Cambridge [etc.], 1967.

ToC figure

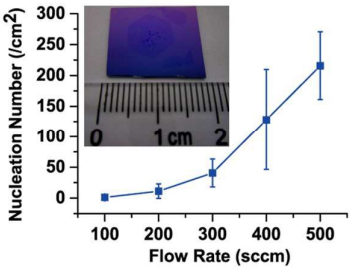

By mildly oxidizing Cu foil and slowing down gas flow rate, centimeter-size single-crystalline graphene was grown on Cu at atmospheric pressure.